Joint International Topical Meeting on Mathematics & Computation and Supercomputing in Nuclear Applications (M&C + SNA 2007)
Monterey, California, April 15-19, 2007, on CD-ROM, American Nuclear Society, LaGrange Park, IL (2007)

CHARACTERISTICS OF SELF-POINT DEFECTS AND THEIR ANISOTROPY MIGRATION IN ELASTIC STRESS FIELDS OF DISLOCATIONS IN FCC Pu

N. A. Dubasova, V. M. Chernov and A. B. Sivak
A.A. Bochvar Institute of Inorganic Materials
123060, P.O. Box 369, Moscow, Russia
chernovv@bochvar.ru

ABSTRACT

Spatial dependence of the elastic interaction energy between the self-point defects and the straight edge (<110>{111} and <110>{110}) and screw (Burgers vector ½ <110>) dislocations in FCC Pu was calculated by hybrid method. Elastic fields of dislocations and their interactions with point defects (elastic dipoles) were calculated in the framework of the anisotropic theory of elasticity. Characteristics of point defects (formation and migration energies, relaxation volumes and dipole moment tensors) in the absence of dislocation stress fields were calculated by molecular statics method (MEAM-type interaction potential).

Key Words: δ-Pu, self-point defects, dipole tensor, dislocation, anisotropic theory of elasticity, interaction energy.

1. INTRODUCTION

Stress fields of dislocations (sources of internal stresses) considerably effect on kinetics of point defects determining additional (in comparison with absence of dislocations) features of decay of solid solutions of point defects [1]. In this connection it is important to study the influence of dislocation stress fields on formation and migration energies of vacancies and self-interstitial atoms (SIA) in fcc Pu.

Experimental determination of the point defect characteristics required for calculation of their interaction with stress fields is a hard problem. Computer simulation with use of interatomic interaction potentials properly describing basic physical properties of a material and its defects is an effective tool for investigation of point defect characteristics. Recently progress has been achieved with the modified embedded atom method (MEAM) for pure Pu [2]. With use of this potential, the formation and migration energies were calculated for vacancy and SIA in fcc Pu [3-5].

In this work, the characteristics (formation and migration energies, relaxation volume and dipole tensor) of self point defects (vacancy, SIA) in stable and metastable (including saddle point) configurations were calculated by molecular statics with use of MEAM interatomic potential. The calculation of dislocations stress fields and their interaction energies with self-point defects were calculated in the frameworks of the anisotropic linear theory of elasticity. The use of the anisotropic theory of elasticity is necessary since fcc Pu is strongly elastically anisotropic material (anisotropy factor of this material is equal to 7 [6]).

2. THE CHARACTERISTICS OF SELF-POINT DEFECTS

Model crystallite with fixed boundary conditions containing ~ 10^3 movable atoms was used for calculation of formation energies E^F, relaxation volumes V^R and dipole tensors P_{ij} (i, j = 1, 2, 3, define the coordinate axes in crystallographic coordinate system) of vacancies and SIA in stable and metastable (including saddle point) configurations. Crystallite consists of three regions: inner (I), intermediate (II) and external (III). The atoms located in region I were movable. The atoms in regions II and III were fixed. Region III is necessary to nullify the forces acting upon the atoms of region II in the perfect crystal. Interatomic interactions in model crystallite were described with potential [2,7] constructed in the framework of the modified embedded atom method (MEAM) [8]. In this work potential parameter set was used with t(3) = 0 [4]. The fcc phase of Pu is stable at zero temperature with such parameter set. In the real Pu the fcc phase is stabilized by adding a small amount of Ga, for example [9,10].

The formation energy of a point defect E^F was defined as

$$E^F = E_{def} - N\cdot(-E_s), \tag{1}$$

where E_{def} is the full energy of crystallite after relaxation, N is the number of atoms in the crystallite with defect, E_s is the sublimation energy.

A point defect in a crystal lattice causes surrounding atoms to be displaced from their ideal positions, thus determining the configuration of the elastic dipole produced in the lattice and characterized by dipole tensor $\{P_{ij}\}$ [11, 12]:

$$P_{ij} = \sum_k R_i^k F_j^k , \tag{2}$$

where R_i^k are Cartesian coordinates (axes along edges of a cubic elementary cell) of radius-vector $\vec{R}^k$ of k-th atom; F_j^k are Cartesian projections of force $\vec{F}^k$ acting on k-th atom from atoms of region I containing the relaxed defect configuration. The summation in Eq. (2) is over the atoms from region II.

As the symmetry of occurred elastic dipole configuration below the local symmetry of the crystal lattice, there are n possible crystallographically equivalent orientations (Table I) of elastic dipoles for the given type of symmetry. Identifications of these orientations are listed in Table I.

The tensor $\{P_{ij}\}$ is represented in terms of the three eigenvalues $P^{(s)}$ (s = 1, 2, 3) and eigenvectors $\mathbf{e}^{(s)}$ since the principal axes $\mathbf{e}^{(s)}$ are completely determined by the local symmetry of the defect configuration.

The relaxation volume V^R has the following connection with dipole tensor [12]:

$$V^R = TrP/3B , \tag{3}$$

where $B = (C_{11} + 2C_{12})/3$; C_{11} and C_{12} are elastic constants, $TrP = P_{11} + P_{22} + P_{33}$.

Table I. Correspondence of orientations (A - F) of elastic dipoles to the crystallographic directions in a cubic crystal for different types of symmetry of point defects

n	A	B	C	D	E	F
3	[100]	[010]	[001]	—	—	—
4	[111]	$[\bar{1}11]$	$[1\bar{1}1]$	$[11\bar{1}]$	—	—
6	[110]	$[\bar{1}10]$	[011]	$[01\bar{1}]$	[101]	$[\bar{1}01]$

Table II lists calculated characteristics of self-point defects in fcc Pu (δ-Pu). Symmetry and number of possible crystallographically equivalent orientations for the considered elastic dipoles are also indicated in Table II.

Table II.The formation energy E^F (eV), the relaxation volume V^R (in atomic volumes), eigenvalues $P^{(s)}$ (eV) and eigenvectors $e^{(s)}$ (s = 1, 2, 3) of the dipole tensor $\{P_{ij}\}$ for different configurations of self-point defects in fcc Pu

Self-point defect	E^F	V^R	$P^{(1)}$	$P^{(2)}$	$P^{(3)}$	$e^{(1)}$	$e^{(2)}$	$e^{(3)}$	Symmetry	*n*
Vacancy	0.53	-0.24	-1.11	-1.11	-1.11	(1 0 0)	(0 1 0)	(0 0 1)	Spherical	1
Vacancy saddle point	2.08	0.22	-0.68	3.40	0.37	(1 1 0)	(-1 1 0)	(0 0 1)	Orthorhombic	6
<100> dumbbell	1.66	1.46	7.53	6.46	6.46	(1 0 0)	(0 1 0)	(0 0 1)	Tetragonal	3
<100> dumbbell saddle point	1.77	1.32	4.98	5.79	7.69	(1 1 0)	(-1 1 0)	(0 0 1)	Orthorhombic	6
Octahedral interstitial	1.82	1.21	5.61	5.61	5.61	(1 0 0)	(0 1 0)	(0 0 1)	Spherical	1
<110> dumbbell	2.19	1.53	18.36	-3.56	6.54	(1 1 0)	(-1 1 0)	(0 0 1)	Orthorhombic	6
Crowdion	2.75	1.56	22.32	-3.43	2.95	(1 1 0)	(-1 1 0)	(0 0 1)	Orthorhombic	6
<111> dumbbell	2.39	1.32	19.96	-3.87	2.30	(1 1 1)	(1 1 -2)	(-1 1 0)	Trigonal	4
Tetrahedral interstitial	2.47	1.97	12.51	7.54	7.54	(1 0 0)	(0 1 0)	(0 0 1)	Spherical	1

The stable SIA configuration is <100> dumbbell. The most energetically favorable SIA migration mechanism is an <100> dumbbell jump to the nearest neighbor lattice site with 90° rotation of its axis (the migration energy 0.11 eV). The vacancy migration energy equals to 1.56 eV. Elastic dipoles corresponding to the saddle point configurations of <100> dumbbell and vacancy have 6 possible equivalent orientations (orthorhombic symmetry).

3. ELASTIC STRESS FIELDS OF DISLOCATIONS

Stress fields σ_{ij}^d of straight edge (ED) and screw (SD) dislocations were calculated within the anisotropic linear theory of elasticity [13]. Elastic constants C_{11}, C_{12}, C_{44} and lattice constant *a*

used for calculation of dislocation stress fields are in accordance with values provided by used above interatomic potentials: C_{11} = 36.42 GPa, C_{12} = 26.34 GPa, C_{44} = 33.65 GPa, a = 0.4638 nm. Table III lists designations and crystallographic characteristics of the considered dislocations.

Table III. Designations and crystallographic characteristics of the considered dislocations

Dislocation	Burgers vector b	Slip plane	Dislocation direction ξ	Angle between vectors b and ξ
SD<110>	$a/2[110]$	arbitrary	$[110]$	0^o
ED<110>{111}	$a/2[110]$	$(\bar{1}11)$	$[\bar{1}1\bar{2}]$	90^o
ED<110>{110}	$a/2[110]$	$(\bar{1}10)$	$[00\bar{1}]$	90^o
SD – Screw Dislocation; ED – Edge Dislocation.				

4. INTERACTION OF DISLOCATIONS WITH POINT DEFECTS

4.1. The Interaction Energy of Dislocations with Point Defects

The formation energy of a point defect in the neighborhood of a dislocation can be written as

$$E_d^F = E^F + E_{int}(\vec{r}), \tag{4}$$

where E^F is the formation energy of the point defect in absence of dislocation, $\vec{r}$ is the radius-vector of the point defect position in relation to the dislocation line. The interaction energy E_{int} of dislocations with point defects (elastic dipoles) within the limits of the linear theory of elasticity can be presented in the form of [14-16]:

$$E_{int}(\vec{r}) = -\ P_{ij}\varepsilon_{ij}^d(\vec{r}) = -P_{ij}S_{ijkl}\sigma_{kl}^d(\vec{r}) = E_0\frac{b}{r}f(\varphi),\quad \int_0^{2\pi}[f(\varphi)]^2 d\varphi = \pi, \tag{5}$$

where r and φ are the point defect coordinates in the polar coordinate system centered at the dislocation line, φ is counted from the dislocation slip plane; ε_{ij}^d is the elastic strain tensor cause by a dislocation; S_{ijkl} is the tensor of crystal elastic compliances; E_0 is the binding energy of a dislocation with point defect (an elastic dipole); $f(\varphi)$ is the function defining angular dependence of the interaction energy; b is the module of dislocation Burgers vector.

Table IV lists the binding energy E_0 of dislocations with point defects calculated for all orientations (Table I) of considered point defect configurations (Table II) and dislocations (Table III). As one can see from Table IV, the value of E_0 significantly depends on dislocation type, configuration and orientation of a point defect.

Table IV. The binding energy E_0 of dislocations with different point defect configurations in fcc Pu, eV

Self-point defect	Orientation	Dislocation		
		ED<110>{111}	SD<110>	ED<110>{110}
Vacancy	-	0.121	0	0.105
Vacancy saddle point	A	0.056	0	0.074
	B	0.337	0	0.279
	C	0.129	0.191	0.157
	D	0.236	0.191	0.157
	E	0.236	0.191	0.157
	F	0.129	0.191	0.157
<100> dumbbell	A	0.777	0.137	0.675
	B	0.777	0.137	0.675
	C	0.681	0	0.609
<100> dumbbell saddle point	A	0.516	0	0.480
	B	0.577	0	0.536
	C	0.776	0.297	0.691
	D	0.757	0.297	0.691
	E	0.757	0.297	0.691
	F	0.776	0.297	0.691
Octahedral interstitial	-	0.609	0	0.529
<110> dumbbell	A	1.705	0	1.511
	B	0.250	0	0.398
	C	1.064	0.775	0.667
	D	1.091	0.775	0.667
	E	1.091	0.775	0.667
	F	1.064	0.775	0.667
Crowdion	A	2.224	0	1.843
	B	0.383	0	0.462
	C	1.536	1.226	1.053
	D	0.873	1.226	1.053
	E	0.873	1.226	1.053
	F	1.536	1.226	1.053
<111> dumbbell	A	1.148	0.232	0.984
	B	0.853	0	0.754
	C	0.902	0	0.754
	D	1.148	0.232	0.984
Tetrahedral interstitial	-	1.056	0	0.916

4.2. Change of Stable SIA Configuration in the Neighborhood of Dislocations

The point defect configuration that occurs in the neighborhood of a dislocation should have the lowest formation energy E_d^F. <100> dumbbell has the lowest formation energy in the absence of dislocation stress fields. In the nearest neighborhood of all considered dislocations there are regions where the formation energy of <110> dumbbell is less than the formation energy of <100> dumbbell. The region boundaries are within the range of (1-2) *b* from a dislocation line.

4.3. Migration of Self-point Defects in the Neighborhood of Dislocations

Each orientation of an elastic dipole respondent to a point defect saddle point configuration corresponds to a certain migration direction. Thus, calculating with use of Eqs. (4,5) formation energies of all possible orientations of the defect saddle point configuration at some point $\vec{r}$, we can determine the point defect migration direction with the lowest migration energy at this point and plot migration pathways along which the migration of the point defect has the lowest energy barriers. Calculated migration pathways of the self-point defects with the lowest energy barriers in dislocation stress fields are shown at Fig. 1. To characterize distances at which anisotropic migration becomes significant, we calculated average distances $\bar{r}$ to the dislocations, at which difference between migration energies of the self-point defects in different directions is larger than value of k_BT (k_B is Boltzmann's constant) at $T = 20$ °C. For all types of considered dislocations and self-point defects $\bar{r}$ equals ~13 b.

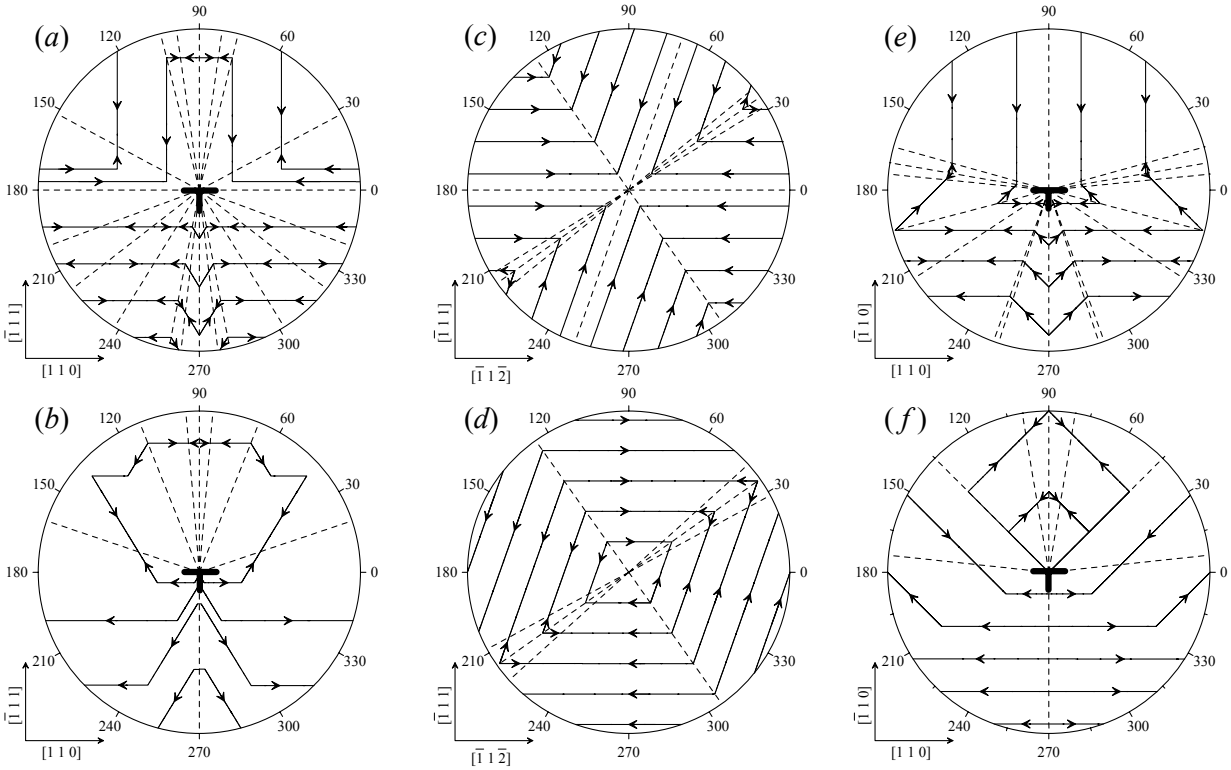

Figure 1. Migration pathways of the self-point defects with the lowest energy barriers in dislocation stress fields (arrows show the direction of the self-point defect motion along the pathway; dotted lines are rays φ = const corresponding to turning points at the defect migration along the pathway):

(*a*) ED<111>{110}, vacancy; **(*b*) ED<111>{110}, <110> dumbbell;**
(*c*) SD<110>, vacancy; **(*d*) SD<110>, <110> dumbbell;**
(*e*) ED<110>{110}, vacancy; **(*f*) ED<110>{110}, <100> dumbbell.**

4.3.1. ED<110>{111} dislocation

In the vacancy attractive region in the angle ranges $200° < \varphi < 218°$, $238° < \varphi < 259°$, $281° < \varphi < 302°$, $322° < \varphi < 340°$ (Fig. 1(*a*)), the migration directions with the lowest migration energy are directed outwards from the dislocation which makes it difficult for the vacancy to approach the dislocation.

For the <110> dumbbell attractive region, the pathways do not lead to the dislocation, which makes it difficult for the SIA to approach the dislocation (Fig. 1(*b*)).

4.3.2. SD<110> dislocation

In the angle ranges $31° < \varphi < 39°$ and $211° < \varphi < 219°$ (Fig. 1(c)), the migration directions of a vacancy with the lowest migration energy are directed outwards from the dislocation. Therefore the pathways lead to the dislocation if vacancy initial position is located in the angle ranges $71° < \varphi < 180°$ or $251° < \varphi < 360°$.

The pathways of the SIA do not lead to the dislocation in the whole angle range, which makes it difficult for the SIA to approach the dislocation (Fig. 1(*d*)).

4.3.3. ED<110>{110} dislocation

In the vacancy attractive region in the angle range $213° < \varphi < 327°$ (Fig. 1(*e*)), the migration directions with the lowest migration energy are directed outwards from the dislocation which makes it difficult for the vacancy to approach the dislocation.

In the <100> dumbbell attractive region in the angle ranges $45° < \varphi < 81°$ and $99° < \varphi < 135°$ (Fig. 1(*f*)), the migration directions with the lowest migration energy are directed outwards from the dislocation, which makes it difficult for the SIA to approach the dislocation.

3. CONCLUSIONS

The characteristics (formation and migration energies, relaxation volume, and dipole tensor) of stable and metastable (including saddle point) self-point defect configurations in fcc Pu crystal were calculated by molecular statics with use of the interatomic potential developed in the framework of the modified embedded atom method.

The most energetically favorable configuration of an self-interstitial atom (SIA) in the absence of the dislocation stress fields is <100> dumbbell with the formation and migration energies equal to 1.66 eV and 0.11 eV, correspondingly. The formation and migration energies of vacancy are 0.53 eV and 1.56 eV, correspondingly.

Interaction energies of self-point defects (elastic dipoles) with edge and screw dislocations in slip systems <110>{111} and <110>{110} in fcc Pu were calculated by methods of the anisotropic theory of elasticity.

Significant influence of dislocation stress fields on the energy and crystallographic characteristics of point defects and directions of their migration is shown. In the nearest neighborhood of all considered dislocations there are regions where the formation energy of <110> dumbbell is less than the formation energy of <100> dumbbell. The region boundaries are within the range of (1-2) *b* from a dislocation line.

Self-point defects migration to the dislocations is impeded for all considered self-point defects and dislocations since the migration directions of self-point defects with the lowest migration energy are directed outwards from the dislocations. The only exception is the case of vacancy migration in the stress field of the screw dislocation.

Average distance to the dislocations, at which difference between migration energies of the self-point defects in different directions is larger than value of k_BT at 20°C, equals ~13 *b* and does not significantly vary depending on the dislocation type and self-point defect configuration.

Indicated features of self-point defects behavior in dislocation fields can exert a significant influence on point defect characteristics and the efficiency of the dislocations as sinks for self-point defects and, consequently, on evolution of material microstructure under damage irradiation (swelling, creep, etc).

ACKNOWLEDGMENTS

The present work was funded by Russian Foundation for Basic Research (project RFBR 05-02-08128ofi-e).

REFERENCES

1. *Elastic strain fields and dislocation mobility*. Eds: V. L.Indenbom and J. Lothe, Amsterdam & North-Holland (1992).
2. M. I. Baskes, “Atomistic model of plutonium,” *Phys. Rev.,* **B62,** pp. 15532-15537 (2000).
3. B. P. Uberuaga, R. G. Hoagland, A. F. Voter, and S. M. Valone, “Atomistic study of vacancy clustering and cluster dynamics in Pu,” *Plutonium Futures – The Science*, California, USA, pp. 517-518 (2006).
4. B. P. Uberuaga, S. M. Valone, M. I. Baskes, and A. F. Voter, “Accelerated molecular dynamics study of vacancies in Pu,” *Plutonium Futures – The Science*, Mexico, USA, July 6–10, pp. 213-215 (2003).

5. S. M. Valone, M. I. Baskes, and B. P. Uberuaga, "Atomistic Models of Point Defects in Plutonium Metal," *Plutonium Futures – The Science*, Mexico, USA, July 6–10, pp. 216-218 (2003).
6. J. Wong, M. Krisch, D. L. Farber, F. Occelli, A. J. Schwartz, T.-C. Chiang, M. Wall, C. Boro, R. Xu, "Phonon Dispersions of fcc δ-Plutonium-Gallium by Inelastic X-ray Scattering," *Science*, **301,** pp. 1078-1080 (2003).
7. S. M. Valone, M. I. Baskes, M. Stan, T. E. Mitchell, A. C. Lawson, and K. E. Sickafus, "Simulations of low energy cascades in fcc Pu metal at 300 K and constant volume," *J. Nucl. Mater.,* **324**, pp. 41-51 (2004).
8. M. I. Baskes, "Modified embedded-atom potentials for cubic materials and impurities," *Phys. Rev.*, **B46**, pp. 2727-2742 (1992).
9. L. F. Timofeeva, "Some Regularities in Eutectoid Transformations in Binary Systems of Plutonium," *Atomic Energy*, **95**, pp. 540-545 (2003).
10. J. L. Robbins, "Mechanical properties of delta-stabilized Pu-1.0 wt% Ga alloys," *J. Nucl. Mater.*, **324**, pp. 125-133 (2004).
11. H. R. Schober and K. W. Ingle, "Calculation of relaxation volumes, dipole tensors and Kanzaki forces for point defects," *J. Phys. F: Metal Phys.*, **10**, pp. 575 -581 (1980).
12. G. Leibfried, N. Breuer, *Point Defects in Metals,* Springer-Verlag, Berlin & Germany (1978).
13. J. P. Hirth, J. Lothe, *Theory of Dislocations*, McGraw-Hill, New York & USA (1968).
14. J. D.Eshelby, *The Continuum Theory of Lattice Defects*, in: Solid State Physics, Eds: F. Seitz, D. Turnball, Academic Press, New York & USA, **3**, pp. 79–144 (1956).
15. E. Kröner, Kontinuumstheorie der Versetzungen und Eigenspannungen, Springer, Berlin – Göttingen – Heidelberg, 1958.
16. V. M. Chernov, V. V. Ivanov., "The influence of elastic anisotropy on interaction of dislocations with point defects in BCC metals," *Crystal Res. and Technol.*, **19**, p. 747-756 (1984).